

Electronic band structure of low-temperature YB_{12} , YB_6 superconductors and layered YB_2 , MgB_2 diborides

I.R. Shein*, S.V. Okatov, N.I. Medvedeva and A.L. Ivanovskii

Institute of Solid State Chemistry, Ural Branch of the Russian Academy of Sciences, 620219, Ekaterinburg, Russia

Electronic band structure of boron-rich low-temperature superconductors YB_{12} -like dodecaboride YB_{12} and CaB_6 -like hexaboride YB_6 are investigated using the first-principle FLMTO calculations and compared with one for layered YB_2 and the new "medium- T_c " superconductor MgB_2 diborides.

1. Introduction

The discovery of the superconductivity in MgB_2 ($T_C \approx 40$ K) [1] and creation of promising materials based thereon (in the form of single crystals, ceramics, thin films, tapes and wires, see reviews [2,3] have attracted a great deal of interest in superconducting properties of other boron-containing phases.

Comparison between different classes of binary (semi- (M_2B) , mono- (MB) , di- (MB_2) , tetra- (MB_4)) and some highest borides (hexa- (MB_6) , dodeca- (MB_{12}) and MB_{66} -like borides), ternary and quaternary borides (review [3]) shows that the majority of known superconductors (SC) are found among low-boron-containing compounds ($\text{B}/\text{M} \leq 2 - 2.5$), in which B atoms are in the form of isolated groups (atoms) or planar sublattices (boron sheets). The superconducting state is far less typical of highest borides ($\text{B}/\text{M} \geq 6$) having a structure made up of stable polyhedra of boron atoms (octahedra B_6 (MB_6), icosahedra B_{12} (MB_{12}) or their combination (MB_{66})). Among a large number of these boron-rich phases, the low-temperature superconductivity was observed only for eight compounds: MB_6 ($\text{M} = \text{Y}$, La , Th , Nd) and MB_{12} ($\text{M} = \text{Sc}$, Y , Zr , Lu) [3]. It is significant that (i) lower borides of these metals, in particular Sc and Y diborides, are not SC, and (ii) the stable polymorphy of the elemental boron (α - B_{12} , β - B_{105}), which under equilibrium conditions contain the boron polyhedra (icosahedra or "gigantic" icosahedra B_{84}) as structural elements, are semiconductors [4-8]. Only recently it was found that polycrystalline boron (rhombohedral β - B_{105}) transforms from a semiconductor to a superconductor ($T_c \approx 11.2$ K) at about 250 GPa [9]. In this work we calculate the electronic band structures of low-temperature SCs - boron-rich phases YB_{12} and YB_6 - and compare them with two representatives of layered AlB_2 -type diborides, namely the non-superconducting YB_2 and new "medium- T_c " SC MgB_2 . The results obtained are analyzed in terms of (i) electronic bands, (ii) density of states (DOS) and (iii) site-projected l-decomposed DOS near the Fermi energy (E_F) of these borides. The Fermi surfaces for YB_2 and MgB_2 are also presented.

dra or "gigantic" icosahedra B_{84}) as structural elements, are semiconductors [4-8]. Only recently it was found that polycrystalline boron (rhombohedral β - B_{105}) transforms from a semiconductor to a superconductor ($T_c \approx 11.2$ K) at about 250 GPa [9]. In this work we calculate the electronic band structures of low-temperature SCs - boron-rich phases YB_{12} and YB_6 - and compare them with two representatives of layered AlB_2 -type diborides, namely the non-superconducting YB_2 and new "medium- T_c " SC MgB_2 . The results obtained are analyzed in terms of (i) electronic bands, (ii) density of states (DOS) and (iii) site-projected l-decomposed DOS near the Fermi energy (E_F) of these borides. The Fermi surfaces for YB_2 and MgB_2 are also presented.

2. Structures and computational

The basic structural elements of the cubic dodecaboride YB_{12} are stable polyatomic boron clusters with icosahedral symmetry (B_{12}) similar to that in elemental boron. The structure of the UB_{12} type (space group is O_h^5 - $\text{Fm}\bar{3}\text{m}$) is formally described in terms of simple rock-salt lattice, where Y occupies Na sites and B_{12} icosahedra are located in Cl sites, the unit cell contains 52 atoms ($Z = 4$). The atomic positions are 4M (a) $0,0,0$; 48B (i) $\frac{1}{2}, x, x$ ($x = 0.17011$ for our self-consistent calculation).

The role of Y and B_{12} in forming the YB_{12} band structure can be elucidated by removing Y atoms from the lattice entirely and calculating

*E-mail: shein@ihim.uran.ru

this hypothetical "dodecaboride" with an empty Y-sublattice (EB₁₂ - E - structure vacancy) and the icosahedral phase (BB₁₂), which is a result of the Y → B substitution.

Yttrium hexaboride has a CaB₆-type structure (space group is O_h¹-Pm3m). It can be formally described in terms of a simple CsCl lattice, where metal atoms occupy Cs sites, while B₆ octahedra are in Cl sites. The unit cell contains 7 atoms (Z = 1). The atomic positions are M(a) 0,0,0; 6B(f) $\frac{1}{2}, \frac{1}{2}, x$ ($x = 0.19538$ for our self-consistent calculation). There are two different B-B distances for intra- and inter-octahedral B-B bonds.

The crystal structure of layered AlB₂-like Mg and Y diborides (space group is D_{6h}¹-P6/mmm) is of an entirely different. It contains graphite-type boron sheets separated by hexagonal close-packed metal layers. Metal atoms are located at the center of hexagons formed by boron atoms. The unit cell contains 3 atoms (Z = 1). The atomic positions are M (a): 0,0,0; 2B (d): $\frac{1}{3}, \frac{2}{3}, \frac{1}{2}$ and $\frac{2}{3}, \frac{1}{3}, \frac{1}{2}$. AlB₂-type diborides exhibit a strong anisotropy of B-B bond lengths: the inter-plane distances are considerably higher than in-plane B-B distances. Table 1 lists the lattice parameters of the borides under study both taken from experiments [10] and obtained in our structural relaxation calculations.

The electronic band structures of the above-mentioned yttrium and magnesium borides were calculated using codes [11]. This program employs a scalar relativistic self-consistent full-potential linear muffin-tin method (FLMTO) within the local density approximation (LDA) [12] with allowance for correlation and exchange effects [13] by using the generalized gradient approximation (GGA) [14]. The tetrahedron method was used to calculate the density of states.

3. Results and discussion

3.1. YB₁₂

Fig. 1 displays the energy bands of YB₁₂ as compared with the hypothetical "dodecaboride" EB₁₂ with a vacant Y sublattice. For EB₁₂, the total width of the valence band (VB) is 10.32 eV (without quasi-core B2s-type flat bands located

at ~ 14 eV below the Fermi level). It includes two groups of occupied hybrid B2s,2p-like bands (A and B) within the intervals $-10.99 \div -8.83$ and $-8.44 \div 0$ eV, separated by a gap (~ 0.4 eV). The lower bands contain predominately B2s-, and the upper bands - B2p-type contributions. The latter can be separated into three groups depending on the intra-atomic bonds in the crystal. There are two types of bonding B2s,2p states in the spectrum of EB₁₂. The states of the first type (covalent intra-icosahedral B-B interactions, namely three-center bonds on the triangular faces of icosahedra) are responsible for the stabilization of individual B₁₂ polyhedra and depend little on the their packing (B₁₂ sublattice structures) and the interaction of B₁₂ between each other (as well as with second sublattice atoms). They correspond to high k-dispersion bonding bands located below E_F and are similar for BB₁₂ and YB₁₂, see Fig. 1,2.

The states of the second group involve inter-icosahedral interactions. The nonbonding 2s,2p states of boron atoms surrounding the vacant sites in B₁₂ belong to third group. The narrow B' and B'' peaks in DOS correspond to it. These states form, in particular, a set of very flat partially occupied bands near the Fermi level (peak B'') with large effective masses. Consequently, EB₁₂ is a metal similar to α -B₅₀ [7]. As distinct from the stable insulating state of α -B₁₂ [5-8], where all mentioned above bands are fully occupied, the "deficiency" of electrons determining the metal-like properties of the hypothetical EB₁₂ is brought about by structural peculiarities of the modeling B₁₂ crystal. There are "empty spheres" in its bulk on the place of removed Y atoms. This intrinsic hole region accumulates some electrons (0.95 e according to our estimates) leading to partial devastation of the upper boron bands. DOS at the Fermi level ($N(E_F) = 6.177$ eV/cell) consist of mainly B2p component (~ 96 percentage). The spectrum of EB₁₂ contains a wide forbidden band of 1.36 eV (FG, direct transition in X point) comparable with the FG in α -B₁₂ (indirect $\Gamma \rightarrow Z$ gap of $\sim 1.43 - 1.70$ eV [5-8]).

The main differences in band structures of YB₁₂ and EB₁₂ are determined by valence yttrium s,p,d-states hybridized with above mentioned

inter-icosahedra and nonbonding B2p states, peak C Fig. 2. For YB₁₂, the total width of the valence band is 12.98 eV, including two groups of fully occupied hybrid B2s,2p bands of 2.82 and 8.89 eV widths separated by a pseudogap. These bands show the significant dispersion near the Fermi level. We also calculated a hypothetical dodecaboride BB₁₂ (isoelectronic with YB₁₂), where an yttrium atom is replaced by an "additional" boron atom, see Fig. 1. It was found that (i) some s,p- states of the "additional" boron atom are located in the vicinity of E_F ; (ii) the system is of a metal-like character with a rather high density of states at the Fermi level ($N(E_F) = 3.034$ eV/cell), the main contribution being from the B2p states (~ 72 percentage).

As noted above, the experiments were reported recently, in which boron transforms from the usual non-metal to the SC state at high pressures (above 160 GPa), the crystal structure of the SC boron remains unknown [6]. This finding was explained [6] on the basis of the electron-phonon mechanism in the assumption that under high pressure -boron undergoes structural transformations to a simple fcc B having a metal-like energy spectrum, with $N(E_F) = 0.154$ states/eV cell (lattice constant 2.44 Å) and the dominant contributions from the B2p states (~ 60 percentage). According to Table 2, the near-the Fermi level regions of our hypothetical systems EB₁₂ and BB₁₂ have a similar band structure. The former system can be interpreted as a model of elemental boron with a disordered lattice. The latter imitates the role of inter-icosahedral boron atoms in crystal. This allows us to surmise that the observed [9] transition of the rhombohedral β -boron to the superconducting state may be due both to lattice disordering and partial frustration of the initial icosahedral units, when some boron atoms take inter-icosahedral positions as a result of high pressure. Such processes can be more probable than the phase transformation of rhombohedral -boron to the fcc structure proposed in [8] if we take into consideration the high cohesion properties of elemental boron [5-7].

3.2. YB₆

Fig. 1 presents the electronic band structure of Y hexaboride. The 10 occupied energy bands are made up by hybrid B2s,p-states represented the inter- and intra-octahedral B-B bonds. The VB width in YB₆ (without quasi-core B2s band) is about 11.80 eV. The highest fully occupied bands are due to Bp_{x,y}-states formed by inter-octahedral interactions. They have strong dispersion along Γ -X direction due to the formation of hybrid Y-B bonds. The DOS spectrum has two maxima (A and B, Fig. 2), corresponding to hybrid states, formed by covalent B-B bonds inside and between B₆ clusters. This feature is typical for all CaB₆ like hexaborides [15-17].

The partially occupied band contains a considerable contribution from cation states and has also a large wave-vector dependence, which reflects the delocalized character of Yd states forming the bottom of the conductivity band.

It has been indicated that YB₁₂ and YB₆ are the conventional low-temperature phonon-mediated BCS superconductors, review [3]. Thus, the important parameter is the orbital composition of $N(E_F)$. According to our data, the lowering of the transition temperature (7.1 K (YB₆) \rightarrow 4.7 K (YB₁₂)) can be explained by a considerable decrease of contributions of Yd-states to $N(E_F)$ from 0.798 (YB₆ ~ 71 percentage) to 0.538 (YB₁₂, ~ 35 percentage per atom in unit cell, Table 2).

3.3. YB₂ as compared with MgB₂

The electronic structures of layered AlB₂-like Mg and Y diborides are of a completely different, Fig. 3, 4. The peculiarities of the band structure of the SC MgB₂ are due to the B2p states which form four $\sigma(2p_{x,y})$ and two $\pi(p_z)$ bands, Fig. 3. The $E(k)$ dependence for B2p_{x,y} and 2p_z bands differs considerably. For B2p_{x,y} like bands the most pronounced dispersion of $E(k)$ is observed along the direction $k_{x,y}$ (Γ - K of the Brillouin zone (BZ)). These bands are of the quasi two dimensional (2D) type. They form a flat zone along k_z (Γ -A) and reflect the distribution of $\sigma(2p_{x,y})$ states in the boron layers. These states make a considerable contribution to the $N(E_F)$ forming metallic properties of the diboride. E_F is located

in the region of bonding states and, the conductivity of MgB_2 is due to hole carriers. Mg is ionized, the charge transfer takes place in the direction $\text{Mg} \rightarrow \text{B}$. $\text{B}2p_z$ -like bands are responsible for weaker $\pi(p_z)$ interactions. These 3D-type bands have the maximum dispersion in the direction k_z (Γ -A). $\text{Mg}s,p$ and $\text{B}s$ states are admixed to $\text{B}2p$ -like bands near the bottom of the VB and in the conduction band. Therefore the peculiarities of the electronic properties of MgB_2 are associated with the metal-like $2p$ states of boron atoms located in plane nets. These states determine the DOS in the vicinity of the Fermi level and is an important condition for superconductivity in MgB_2 and related phases [2,3, 19-21]. Thus the crucial features of the band spectrum of MgB_2 for its superconducting properties (see also [2,3,19-21]) are: (i) the position of $\sigma(p_{x,y})$ bands relative to E_F (the presence of hole $p_{x,y}$ -states); (ii) their dispersion in the direction Γ - A ($\Delta E^\sigma(\Gamma$ -A) is determined by the interaction between metal-boron layers); (iii) the value and orbital composition of $N(E_F)$ (the main contributions from boron σ -states).

Let us compare the band structures of MgB_2 and YB_2 . The most obvious consequence of the metal variation ($\text{MgB}_2 \rightarrow \text{YB}_2$) is band filling change caused by the increased number of valence electrons. For YB_2 , the Fermi level is shifted towards a pseudogap between bonding and antibonding states. As a result, the near- E_F spectra of YB_2 and MgB_2 differ radically. For YB_2 , (i) $\sigma(p_{x,y})$ boron bands are almost filled and the hole concentration is very small (near point A of the BZ, Fig. 3); (ii) the covalent d-p metal-boron bonding increases considerably and the $\text{B}2p$ -like bands are shifted downwards to point K (these interactions are also responsible for the appearance of pronounced dispersion of bands in the direction $\Gamma \rightarrow$ - A and for $2\text{D} \rightarrow 3\text{D}$ transformation of the near- E_F states); (iii) the Y4d band along the Γ -M is below E_F and these states give a large (~ 59 percentage) contribution to $N(E_F)$.

The $2\text{D} \rightarrow 3\text{D}$ transformation of the near- E_F states can be also traced by comparing the the Fermi surfaces (FS) of MgB_2 and YB_2 , Fig. 3. For MgB_2 , $\text{B}2p_{x,y}$ bands form two hole-like cylindrical Fermi surfaces around the Γ - A direction.

The other tubular surfaces come from bonding (hole-like) and antibonding (electron-like) $\text{B}2p_z$ bands. By contrast, the FS of YB_2 consists of hole-like ellipsoids around the Γ - A line and 3D figures with electron-type conductivity. All these FSs are defined by mixed Y4d- $\text{B}2p$ states. Thus, the absence of superconductivity in YB_2 can be accounted for (see also [21]) by the high energy shift of E_F , a considerable increase of Y4d-component in $N(E_F)$, and the absence of $\sigma(p_{x,y})$ hole states at Γ , Fig. 3.

4. Conclusions

We presented the results of full-potential LMTO band structure calculations for yttrium dodeca- and hexaborides compared with layered non-superconducting YB_2 and the new "medium- T_c " SC MgB_2 diborides.

The band structures of boron-rich crystals are determined by the complicated intraatomic bonds including intra and between boron polyhedra (B_{12} for YB_{12} and B_6 for YB_6) and direct Y-B bonds. The DOS at the Fermi level for the low-temperature SC YB_{12} and YB_6 has a similar composition and includes the large contribution of Y4d-states. The lowering of T_c ($\text{YB}_6 \rightarrow \text{YB}_{12}$) can be explained by a considerable decrease in main contributions of Yd-states to $N(E_F)$. We performed also band structure calculations for two hypothetical structures: "dodecaboride" with an empty Y-sublattice (EB_{12}) and the icosahedral phase (BB_{12}), which is a result of the $\text{Y} \rightarrow \text{B}$ substitution. Both crystals are metals with high DOS at the Fermi level. We speculate that the observed [9] transition of the rhombohedral β -boron to the superconducting state can be due to both lattice disordering and partial frustration of the initial icosahedral units as a result of high pressure. Such processes can be more energetically favorable than the phase transformation of rhombohedral β -boron to the fcc structure proposed in [8].

Quite different are the band structures of layered AlB_2 -like Mg and Y diborides. They are determined by intra- and interlayer interactions of plane (Mg,Y) and boron nets. In contrast to MgB_2 , for YB_2 the increase of covalent d-

p bonding leads to the downward shift of B2p_z bands, larger dispersion of σ bands in the direction Γ - A and 2D \rightarrow 3D band transformation near- E_F . The most crucial changes are connected with the increase of electron numbers resulting in the almost filled $\sigma(p_{x,y})$ boron bands. The hole $\sigma(p_{x,y})$ bands are absent at point and the density of states at the Fermi level is mainly defined by Y4d states, so these band structure peculiarities may be considered to be responsible for the absence of medium- T_c superconductivity in YB₂.

REFERENCES

1. J. Nagamatsu, N. Nakagawa, T. Muranaka, Y. Zenitani, J. Akimitsu, Nature 410 (2001) 63.
2. A.L. Ivanovskii, Russ. Chem. Rev. 70 (2001) 717.
3. C. Buzea, T. Yamashita, Superconductors, Science and Technol. 14 (2001) R115.
4. The Chemistry of Boron and Its Compounds (Ed. E.L. Muetterties), Wiley, New York, 1967.
5. S. Lee, D.M. Bylander, L. Kleinman, Phys. Rev. B42 (1990) 1316.
6. C. Maihiot, J.B. Grant, A.K. McMahan, Phys. Rev. B42 (1990) 9033.
7. D. Li, Y-N. Xu, W.Y. Ching, Phys. Rev. B45 (1992) 5895.
8. D.A.Papaconstantopoulos, M.J. Mehl, Cond-matter/0111385 (2001).
9. M.L. Eremets, V.V. Struzhkin, H.K. Mao, R.J. Hemley, Science 203 (2001) 272.
10. Yu.B. Kuzma, Crystal chemistry of borons (in Russia), Vyssha Shkola, Lviv, 1983.
11. S.Y.Savrasov, Phys. Rev. B54 (1996) 16470.
12. M.Methfessel, M. Scheffler, Physica B. 172 (1991) 175.
13. J. P. Perdew and Y. Wang, Phys. Rev. B45 (1992) 13244
14. J.P. Perdew, S. Burke and M. Ernzerhof, Phys. Rev. Lett. 77 (1996) 3865.
15. H. Hasegawa, A. Yanase, J. Phys. C: Solid State Phys. 12 (1979) 5431.
16. H. Ripplinger, K. Schwarz, P. Blaha, J. Solid State Chem. 133 (1997) 51.
17. S. Massidda, A. Continenza, T. M. DePascale, R. Monnier, Z. Phys. B - Condensed Matter. 102 (1997) 83.
18. A.L. Ivanovskii, S.V. Okatov. Mendeleev Commun. 11 (2001) 8.
19. J.M. An, W.E. Pickett, Phys. Rev. Letters, 86 (2001) 4366.
20. J. Kortus, I.I. Mazin, K.D. Belashenko, V.P. Antropov, L.L. Boyer. Phys. Rev. Letters. 86 (2001) 4656.
21. N.I. Medvedeva, A.L. Ivanovskii, J.E. Medvedeva, A.J. Freeman. Phys. Rev., B64 (2001) 020502(R).

Table 1

Transition temperatures (T_c , K), structure type and lattice constants (\AA) YB_{12} , YB_6 , YB_2 and MgB_2 . a and c are lattice parameters from [10], a^* and c^* are lattice parameters from our self-consistent data.

Boron	T_c	Structure type (space group)	a	c	a^*	c^*
YB_{12}	4.7	$\text{UB}_{12}(\text{Fm}3\text{m})$	7.5000	-	7.5223	-
YB_6	7.1	$\text{CaB}_6(\text{Pm}3\text{m})$	4.1132	-	4.1554	-
YB_2	—	$\text{AlB}_2(\text{P6}/\text{mmm})$	3.3036	3.8427	3.2116	4.0080
MgB_2	~ 40	$\text{AlB}_2(\text{P6}/\text{mmm})$	3.083	3.521	3.0487	3.4664

Table 2

Total and site-projected l - decomposed DOS at the Fermi level (state/eV/cell) for borides.

Boride	Total	Ms	Mp	Md	Bs	Bp
YB_{12}	1.458	0.005	0.003	0.532	0.033	0.885
EB_{12}	6.177	0.240			0.033	5.904
BB_{12}	3.034	0.743	0.119		0.109	2.063
YB_6	1.130	0.017	0.020	0.798	0.001	0.294
YB_2	1.665	0.042	0.106	0.983	0.006	0.528
MgB_2	0.719	0.040	0.083	0.138	0.007	0.448

Figures.

Fig.1. Band structures of YB_{12} (I), EB_{12} (II), BB_{12} (III) and YB_6 (IV).

Fig.2. Total and partial DOS (1- s, 2 - p, 3 - d) for YB_{12} , EB_{12} and YB_6 .

Fig.3. Band structure and Fermi surface for YB_2 (I) and MgB_2 (II).

Fig.4. Total and partial DOS (1-s, 2 - p, 3 - d) for YB_2 (I) and MgB_2 (II).

1

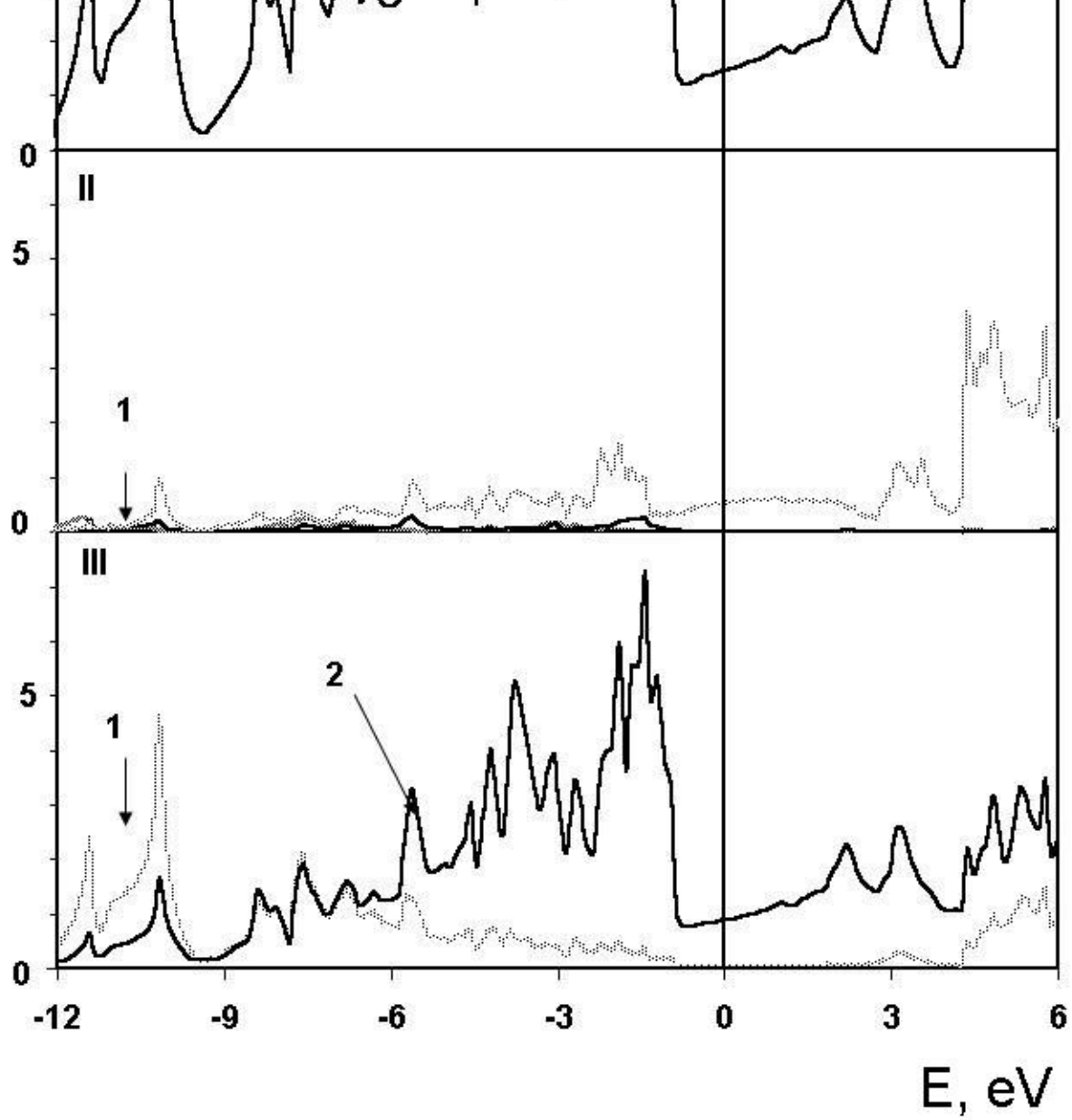
X

W

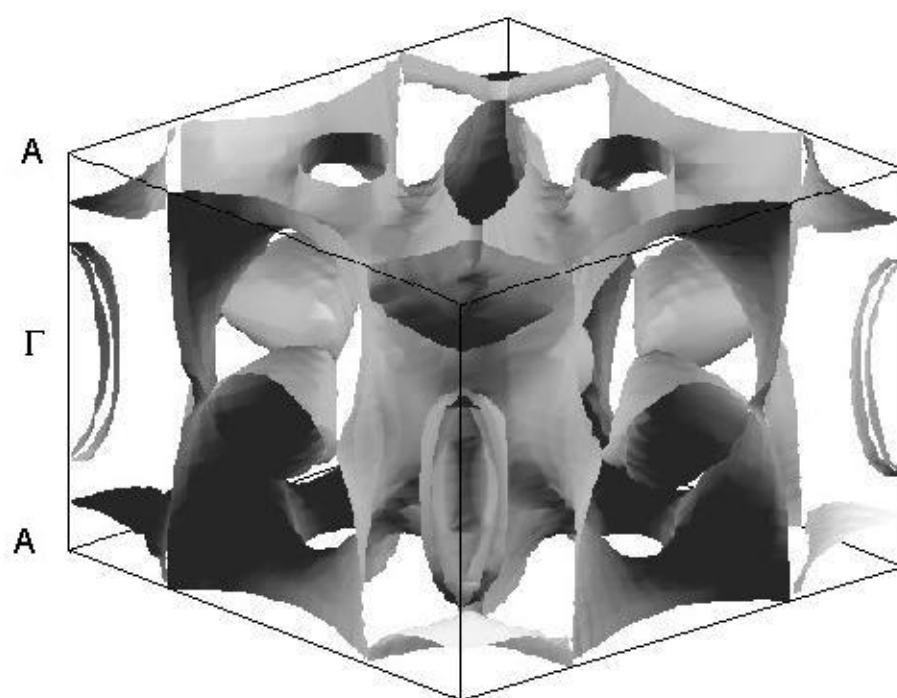
X

K

1



-12 Γ M K Γ A L H A



-12 Γ M K Γ

